

1 **Reduced-complexity air quality intervention modelling**
2 **over China: development of the InMAPv1.6.1-China and**
3 **comparison with the CMAQv5.2 model**

4 Ruili Wu¹, Christopher W. Tessum², Yang Zhang³, Chaopeng Hong⁴, Yixuan Zheng⁵,
5 Qiang Zhang¹

6 ¹Ministry of Education Key Laboratory for Earth System Modelling, Department of Earth System
7 Science, Tsinghua University, Beijing 100084, China

8 ²Department of Civil and Environmental Engineering, University of Illinois at Urbana-Champaign,
9 Urbana, Illinois 61801, United States

10 ³Department of Civil and Environmental Engineering, Northeastern University, Boston, Massachusetts
11 02115, United States

12 ⁴Department of Earth System Science, University of California, Irvine, California 92602, United States

13 ⁵Center of Air Quality Simulation and System Analysis, Chinese Academy of Environmental Planning,
14 Beijing 100012, China

15 Correspondence to: Ruili Wu (wurl15@mails.tsinghua.edu.cn),

删除的内容: (wurl15@tsinghua.org.cn)

16 **Abstract.** This paper presents the first development and evaluation of the reduced-complexity air quality
17 model for China. In this study, a reduced-complexity air quality intervention model over China (InMAP-
18 China) is developed by linking a regional air quality model, a reduced-complexity air quality model, an
19 emission inventory database for China, and a health impact assessment model to rapidly estimate the air
20 quality and health impacts of emission sources in China. The modelling system is applied over mainland
21 China for 2017 under various emission scenarios. A comprehensive model evaluation is conducted by
22 comparison against conventional CMAQ simulations and ground-based observations. We found that
23 InMAP-China satisfactorily predicted total PM_{2.5} concentrations in terms of statistical performance.
24 Compared with the observed PM_{2.5} concentrations, the mean bias (MB), normalized mean bias (NMB),
25 and correlations of the total PM_{2.5} concentrations are -8.1 µg/m³, -18%, and 0.6, respectively. The
26 statistical performance is considered to be satisfactory for a reduced-complexity air quality model and
27 remains consistent with that evaluated in the United States. The underestimation of total PM_{2.5}
28 concentrations was mainly caused by its composition, primary PM_{2.5}. In terms of the ability to quantify
29 source contributions of PM_{2.5} concentrations, InMAP-China presents similar results in comparison with
30 those based on the CMAQ model, the difference is mainly caused by the different treatment of secondary

删除的内容: mechanism and the

33 inorganic aerosols in the two models. Focusing on the health impacts, the annual PM_{2.5}-related premature
34 mortality estimated using InMAP-China in 2017 was 1.92 million, which was 25 ten thousand deaths
35 lower than that estimated based on CMAQ simulations as a result of underestimation of PM_{2.5}
36 concentrations. This work presents a version of the reduced-complexity air quality model over China,
37 provides a powerful tool to rapidly assess the air quality and health impacts associated with control policy,
38 and to quantify the source contribution attributable to many emission sources.

39 1 Introduction

40 With rapid urbanization and industrialization, fine particulate matter pollution less than 2.5 μm in
41 diameter (PM_{2.5}) has become a major environmental issue in China. High PM_{2.5} concentrations can be
42 observed over eastern China from satellite observations (Xiao et al., 2020) and the PM_{2.5} concentrations
43 have been largely decreased since 2013 due to the effective control measures taken by Chinese
44 governments (Zhao et al., 2021). PM_{2.5} can affect air quality, ecosystems, and climate change and damage
45 human health through short-term or long-term exposure. The Global Burden of Disease study reported
46 that 1.1 million premature deaths were caused by long-term PM_{2.5} exposure over China in 2015 (Cohen
47 et al., 2017).

48 State-of-the-science three-dimensional air quality models (AQMs) have been widely used in China
49 as tools to simulate regional PM_{2.5} concentrations, quantify the contributions to total PM_{2.5} concentrations
50 resulting from emission sources and assess the benefits associated with control measures (Chang et al.;
51 2019, Li et al., 2015; Zhang et al., 2015; Zhang et al., 2019). The Weather Research and Forecasting
52 model-Community Multiscale Air Quality Modelling System (WRF-CMAQ) (Appel et al., 2017; Chang
53 et al., 2019), the Weather Research and Forecasting model coupled with Chemistry (WRF-Chem)
54 (Reddington et al., 2019), the Weather Research and Forecasting model-Comprehensive Air Quality
55 Model Extension (WRF-CAMx) (Li et al., 2015), and the Global Adjoint model of Atmospheric
56 Chemistry (GEOS-Chem Adjoint) (Zhang et al., 2015) were frequently used in previous studies. To
57 conduct a series of simulations for multiple scenarios or quantify the separate contributions attributable
58 to multiple sources, large computational resources and run time are required while utilizing conventional
59 AQMs. To address these challenges, and to improve the availability and accessibility of air quality
60 modelling, a number of reduced-complexity models have been developed by the air quality research
61 community. The three representative reduced-complexity air quality models frequently used are the

批注 [吴瑞丽1]: Statement: the revised sentences are marked in red.

批注 [吴瑞丽2]:

删除的内容: (Xiao et al., 2020) and the PM_{2.5} concentrations have been largely decreased since 2013 due to the effective control measures taken by Chinese governments (Zhao et al., 2021)

删除的内容: State-of-the-science three-dimensional air quality models (AQMs)

删除的内容: The Weather Research and Forecasting model-Community Multiscale Air Quality Modelling System (WRF-CMAQ) (Appel et al., 2017; Chang et al., 2019), the Weather Research and Forecasting model coupled with Chemistry (WRF-Chem) (Reddington et al., 2019), the Weather Research and Forecasting model-Comprehensive Air Quality Model Extension (WRF-CAMx) (Li et al., 2015), and the Global Adjoint model of Atmospheric Chemistry (GEOS-Chem Adjoint)

删除的内容: AQMs

删除的内容: these challenges

79 Estimating Air Pollution Social Impacts Using Regression (EASIUR) model (Heo et al., 2016; Heo et
80 al., 2017), the updated Air Pollution Emission Experiments and Policy (APEEP2) model (Muller et al.,
81 2007; Muller et al., 2011) and the Intervention for Air Pollution model (InMAP) (Tessum et al., 2017).
82 A recent study compares three reduced-complexity models, EASIUR, APEEP2, and InMAP, and the
83 results indicate that these three models are consistent in their assessment of the marginal social cost at
84 the county level (Gilmore et al., 2019). Reduced-complexity air quality models are less computationally
85 intensive and easier to use. However, it is not available for China. Therefore, it is essential to develop a
86 reduced-complexity air quality model over China to quickly predict PM_{2.5} concentrations and the
87 associated health impacts of emission sources.

88 The reduced-complexity intervention model for air pollution, InMAP, was developed by Tessum et
89 al. (Tessum et al., 2017) to rapidly assess the air pollution, health, and economic impacts resulting from
90 marginal changes in air pollutant emissions. Compared with conventional air quality models, InMAP has
91 the advantage of time efficient, can predict annual-average PM_{2.5} concentrations within few hours but
92 with a modest reduction in accuracy compared with CTMs. InMAP reduces the running time by
93 simplifying the physical and chemical process. InMAP has been used to assess marginal health damage
94 of location-specific emission sources (Goodkind et al., 2019), to quantify the health impacts of individual
95 coal-fired power plants in the United States (Thind et al., 2019) and to estimate the health benefits of
96 control policies considering specific locations (Sergi et al., 2020). However, to date, a version of the
97 reduced-complexity air quality intervention model over China is absent.

98 In this work, based on the source code of the version 1.6.1 of InMAP model, a reduced-complexity
99 air quality intervention model over China (InMAP-China) is developed to rapidly predict the air quality
100 and estimate the health impacts of emission sources in China. The modelling system is applied over
101 mainland China for 2017 under various emission scenarios to examine model performance. Comparisons
102 against conventional air quality models and surface observations are performed in this study. The model
103 applicability and limitations are also declared.

104 The paper is organized as follows: Section 2.1 presents the components of InMAP-China including
105 the interface development between WRF-CMAQ and InMAP to generate parameters of the base
106 atmospheric state, the preprocessed process of emission input data and the exposure-response functions
107 employed in this model. Section 2.2 introduces the evaluation protocol, including the statistical variables
108 adopted and the simulation design in this study. Section 3 presents the evaluation of InMAP-China's

批注 [吴瑞丽4]:

Line 78: InMAP should be spelled out when it is firstly
used in the paper.

Spelled out in Line 80.

删除的内容: including

110 predictions of PM_{2.5} air quality and PM_{2.5}-related health impacts in several simulations. Section 4
111 summarizes the conclusions and limitations of this study.

112 2 Description of InMAP-China model

113 2.1 Model components and configurations

114 The reduced-complexity intervention model for air pollution, InMAP, was developed by Tessum et
115 al. (Tessum et al., 2017) to rapidly assess the air pollution, health, and economic impacts resulting from
116 marginal changes in air pollutant emissions. The model has been widely used in studies (Sergi et al.,
117 2020; Thind et al., 2019; Goodkind et al., 2019; Dimanchevi et al., 2019) focusing on PM_{2.5} pollution
118 and health, economic impacts resulting from emission sources in the United States. In this model, the
119 continuous equation of atmospheric pollutants is solved at an annual scale, and the run time can be
120 reduced. The parameters used to represent physical and chemical processes for simplified simulation are
121 calculated prior to using CTM output data. PM_{2.5} air quality and PM_{2.5}-related premature mortality are
122 predicted and output in the InMAP model.

123 In this work, a Chinese version of the reduced-complexity air quality intervention model InMAP-
124 China is developed for the purpose of rapidly estimating the PM_{2.5} concentration and associated health
125 impacts of emission sources. ~~Figure 1 shows the model framework. Based on the source code of the~~
126 InMAP model, three-step development work is conducted to establish InMAP-China. First, we develop
127 a preprocessed interface to calculate physical and chemical process parameters using the WRF-CMAQ
128 output variables to support the simplified simulation in InMAP-China. Second, air pollutant emission
129 data are preprocessed to an appropriate format for the InMAP-China simulation. Third, the exposure-
130 response function of the GEMM model is employed in InMAP-China and replaces the original default
131 function to assess PM_{2.5}-related health impacts.

132 Table 1 presents the basic configurations of InMAP-China. The simulation domain is over East
133 Asia and covers mainland China. The spatial resolution is 36 km. Fourteen vertical layers are used in
134 InMAP-China, ranging from the surface layer to the top level of the tropospheric layer.

135 2.1.1 Parameter interface development for simplified simulation in InMAP-China

136 We develop a preprocessed interface to calculate physical and chemical process parameters using
137 WRF-CMAQ output variables for simplified simulation in InMAP-China based on the Environmental
138 Protection Agency's (EPA) work (Baker et al., 2020). The main step of the preprocessed interface

删除的内容: Figure 1 shows the model framework.

140 includes meteorological and chemical variable extraction and merging, unit conversion, vertical layer
141 mapping, physical and chemical process parameter calculation and average processing. The hourly
142 chemical and meteorological variable outputs from the WRF-CMAQ modelling system are converted
143 into annual-average physical and chemical process parameters required for simplified simulation.

144 A NETCDF file containing the three-dimensional annually averaged parameters to characterize
145 atmospheric advection, dispersion, mixing, chemical reaction, and deposition is generated. Table 2 shows
146 the relationship between the annual-average parameters for simplified simulation and the original hourly
147 variables. In InMAP-China, the annual averaged component and the deviation of wind speed to represent
148 advection are calculated using hourly elements. The offset of wind vectors in different directions may
149 result in some uncertainties in this process. The parameters of eddy diffusion and convective transport
150 are precalculated using hourly elements, including temperature, pressure, boundary layer height, etc. The
151 annual wet deposition rate is determined by the rainwater mixing ratio and cloud fractions. The annual
152 dry deposition rate of particles and gaseous pollutants at the surface level is precalculated using friction
153 speed, heat flux, radiation flux and land cover.

154 The simplification of chemical reactions is different among pollutants. For NO_x, NH₃, and volatile
155 organic compound (VOC) precursors, the annual averaged gas-particle partitioning is adopted and
156 calculated before using the output concentrations of species from CMAQ. For SO₂ pollutants, the annual
157 oxidation rate of two major conversion pathways for SO₂ is calculated using concentrations of hydroxyl
158 radical (HO) and hydrogen peroxide (H₂O₂) in CMAQ, and the conversion is estimated in InMAP-China.

159 **2.1.2 Prior WRF-CMAQ simulation**

160 To generate the meteorological and chemical parameters required by InMAP-China, a one-year
161 WRF-CMAQ simulation is conducted to output hourly meteorological and chemical-related variables in
162 the year 2017. Tables S1 and S2 show the major configurations of the WRF-CMAQ modelling system.
163 The WRF model is driven by the National Centers for Environmental Prediction Final Analysis (NCEP-
164 FNL) (<https://doi.org/10.5065/D6M043C6>) reanalysis data to provide the initial and boundary conditions.
165 The meteorological fields derived from the WRF model is used to drive the CMAQ model (Appel et al.,
166 2016) simulations. The air pollutant emissions used here include anthropogenic emissions over China
167 derived from the MEIC model (<http://meicmodel.org/>), anthropogenic emissions over the region of East
168 Asia outside China derived from the MIX-2010 inventory (Li et al., 2015), and biogenic emissions
169 derived from the MEGANv2.10 model. The CB05 chemical mechanism and the AERO6 aerosol module
170 are employed in the model simulation.

171 Table S3 summarizes the performance statistics of meteorological variables, including surface
172 temperature, relative humidity, and wind speed, in China in 2017, as simulated by the WRF model. The
173 hourly observed data of major meteorological variables derived from the National Climate Data Center
174 (NCDC) are utilized here. The results show that the meteorological variables simulated by the WRF
175 model agree well with the surface observations, which is consistent with previous studies (Wu et al.,
176 2019; Zheng et al., 2015; Hong et al., 2017). The model performs well on the predictions of surface
177 temperature, with an MB of -0.7 K, an NMB of -6.1%, and R of 0.9. The predictions of relative humidity
178 at a height of 2 metres are relatively satisfied with an MB of 4.1% and an NMB of 6.1%. The predictions
179 of wind speed at a height of 10 metres are slightly overestimated, with an MB of 0.3 m/s and an NMB
180 of 12.4%, which may be caused by out-of-date USGS land use data employed in the model runs.

181 The SO₂, NO₂ and PM_{2.5} concentrations modelled across the domain agree well with the surface
182 observations in terms of the statistical performance and monthly variations. Table S4 summarizes the
183 performance of the statistics of major air pollutant concentrations. The nationwide annual averaged PM_{2.5}
184 concentration simulated in 2017 in China was 42.1 µg/m³. Compared with the observed PM_{2.5} of 45.9
185 µg/m³, there are slight underpredictions with an MB of 3.7 µg/m³ and NMB of 8.1%. The CMAQ model
186 has moderate underpredictions of the NO₂ concentrations and SO₂ concentrations, which may be related
187 to the uncertainties of emission inputs. For modelled NO₂ concentrations, MB and NMB are -4.6 µg/m³
188 and -13.9%, respectively. For modelled SO₂ concentrations, MB and NMB are -0.8 µg/m³ and -4.5%,
189 respectively. Figure S3 shows the monthly variation. The variation trend of the observed SO₂, NO₂, and
190 PM_{2.5} concentrations can basically be reproduced in the CMAQ simulations.

191 2.1.3 Preprocessed emission input data

192 Additionally, we develop the preprocessed module to generate vector emission input for the
193 InMAP-China simulation. This module can allocate air pollutant emissions vertically and horizontally to
194 supply the missing parameters for the emission file and convert them into shapefile vector format. The
195 emission data are preprocessed by source and altitude.

196 The anthropogenic emissions of five sectors in China in 2017 from the MEIC inventory
197 (<http://meicmodel.org/>), the anthropogenic emissions over regions outside mainland China in Asia from
198 the MIX-2010 inventory (Li et al., 2015), and the natural emissions estimated using the MEGANv2.10
199 model (Guenther et al., 2012) are employed in this study. Gridded anthropogenic emissions of 0.3
200 degrees for the residential, transportation, and agricultural sectors are preprocessed and input to the
201 surface layer. The gridded air pollutant emissions of the industrial sector and noncoal power plants are

202 preprocessed for allocation to attitudes ranging from 130 metres to 240 metres and 130 metres to 890
203 metres, respectively.

204 The emissions of coal-fired power plants (CPPs) are preprocessed as point sources. The air pollutant
205 emissions and the stack attribution of each unit are provided in the emission file. Because the stack
206 attribution of the power unit is missed in the MEIC inventory, we supplied the information in the
207 preprocessed module based on NEI (National Emission Inventory data) data of power units. For stack
208 height/stack diameter, a linear relationship is first established (see Figure S1), and then, supplementation
209 for these two parameters of Chinese power plants is conducted by using the relationships. The fixed
210 value for the other two variables of stack attribution is set here because the $PM_{2.5}$ concentrations
211 attributable to power plants (CPPs- $PM_{2.5}$) are less sensitive to the two variables (see Figure S2). The
212 stack gas exit velocity and stack gas exit temperature of the power unit are 6 m/s and 313 K, respectively.

213 The air pollutant emissions over regions outside mainland China in Asia and the natural emissions
214 simulated by MEGANv2.10 are preprocessed and input to the surface layer.

215 **2.1.4 Exposure-response function from GEMM**

216 In InMAP-China, we employ the exposure-response function from GEMM to estimate $PM_{2.5}$ -related
217 premature mortality, which was developed by Burnett et al. (Burnett et al., 2018). Premature mortality
218 due to noncommunicable diseases (NCDs) and lower respiratory infections (LRIs) was considered in this
219 study. Mortality is determined by the mortality incidence rate, population, and attributable fraction (AF)
220 to certain $PM_{2.5}$ concentrations. The national mortality incidence rate and the population data were derived
221 from the GBD2017 study (Institute for Health Metrics and Evaluation). The spatial distribution of the
222 population in 2015 from the Gridded Population of World Version 4 (Doxsey et al., 2015) was employed
223 to allocate the population in 2017.

224 **2.2 Evaluation protocol**

225 **2.2.1 Evaluation method**

226 In this study, the performances of the InMAP-China predictions are evaluated by comparison
227 against CMAQ simulations and surface observations. Model-to-model comparison and model-to-
228 observation comparison have both been used to evaluate the performance of reduced-complexity air
229 quality models in previous studies (Tessum et al., 2017, Gilmore et al., 2019).

230 The following aspects are considered to make an evaluation. First, we examine the ability of
231 InMAP-China to predict $PM_{2.5}$ concentrations at different emission levels, which will be introduced in

232 Section 3.1. Second, to examine the ability to quantify source contributions to PM_{2.5} concentrations, we
233 compare the InMAP-China's predictions of the sectoral contributions attributable to power, industry,
234 residential, transportation, and agriculture with those based on the CMAQ model, which will be
235 presented in Section 3.2. Third, focusing on the health impacts, the PM_{2.5}-related premature mortality
236 predicted by InMAP-China is also compared with mortality estimation based on PM_{2.5} exposure derived
237 from CMAQ, which is presented in Section 3.3.

238 The statistical parameters used in this study include the correlation coefficient (R), mean bias (MB),
239 mean error (ME), normalized mean bias (NMB), normalized mean error (NME), and root mean square
240 error (RMSE). The statistical analyses on the performance of InMAP-China are similar to our previous
241 evaluation of conventional CTMs (Zheng et al., 2015; Wu et al., 2019).

242 The annual averaged observed PM_{2.5} concentrations in 2017 were calculated using hourly
243 concentration data from the China National Environmental Monitoring Center, CNEMC
244 (<http://www.cnemc.cn/>). More than 1400 national monitoring sites for air pollutant concentrations are
245 included in the simulation domain.

246 2.2.2 Experimental design

247 We design eleven simulations to examine the model ability of InMAP-China in this study. Table 3
248 shows the sequence of simulations.

249 InMAP_TOT represents the baseline simulation with maximum emissions input, in which five
250 sectoral anthropogenic emissions derived from the MEIC inventory, natural emissions derived from the
251 MEGANv2.10 model, and Asian emissions outside mainland China derived from the MIX-2010
252 inventory are combined as emission inputs. Five sectoral and five abatement simulations are also
253 conducted to examine the ability of InMAP-China to predict concentration changes in response to
254 sectoral emissions and abatement emissions. The emission inputs for these ten simulations have been
255 declared in Table 3. The annual averaged physical and chemical process parameters are calculated based
256 on the output variables of WRF-CMAQ model, which has already been mentioned in Section 2.1.2.
257 Based on the above input, the particle continuity equations are solved by InMAP-China model to obtain
258 the annual averaged PM_{2.5} concentrations at the steady state of atmosphere.

259 In order to make a comparison with the InMAP-China simulations, eleven CMAQ simulations are
260 also performed under the same emission inputs. The hourly PM_{2.5} concentrations simulated by CMAQ
261 in 2017 are averaged at obtain the annual averaged PM_{2.5} concentrations. Due to limited computational

删除的内容: Five sectoral and five abatement simulations are also conducted to examine the ability of InMAP-China to predict concentration changes in response to sectoral emissions and abatement emissions. The emission inputs for these ten simulations have been declared in Table 3. The annual averaged physical and chemical process parameters are calculated based on the output variables of WRF-CMAQ model, which has already been mentioned in Section 2.1.2. Based on the above input, the particle continuity equations are solved by InMAP-China model to obtain the annual averaged PM_{2.5} concentrations at the steady state of atmosphere.

274 resources, each simulation is conducted for four representative months (January, April, July, and October)
275 in 2017.

276 **3 Results and Discussion**

277 **3.1 Model performance of PM_{2.5} concentrations**

278 **3.1.1 Total PM_{2.5} concentrations**

279 Figure 3 shows the performance evaluation of total PM_{2.5} concentrations in the InMAP_TOT
280 simulations. Compared with the observed annual averaged PM_{2.5} concentrations, the total PM_{2.5}
281 concentrations are moderately underpredicted by InMAP-China with an MB of -8.1 μg/m³ and an NMB
282 of -18.1%. Compared with the CMAQ predictions, the total PM_{2.5} concentrations are also underpredicted,
283 with an MB of -5.3 μg/m³ due to the underprediction of primary PM_{2.5}. Consistent air pollutant emissions
284 are employed in the CMAQ and InMAP-China simulations. Therefore, the underpredictions are caused
285 by the different mechanisms in the two models. Basically, InMAP-China reproduces the spatial pattern
286 of total PM_{2.5} concentrations simulated by CMAQ. Notably, significant overpredictions of PM_{2.5}
287 concentrations can be observed over mountain areas across Northern China, and the complex terrain and
288 large emission intensity increase the challenge of predicting PM_{2.5} concentrations using the reduced-
289 complexity air quality model in this region.

290 Figure 4 shows a comparison of PM_{2.5} compositions. Compared with the CMAQ results, the
291 InMAP-China predictions of PM_{2.5} compositions are satisfactory, with NMBs for SO₄²⁻, NO₃⁻, NH₄⁺, and
292 primary PM_{2.5} equal to 13%, -8%, -10%, and -23%, respectively. The predictions of SO₄²⁻, NO₃⁻, and
293 NH₄⁺ perform better than those of primary PM_{2.5}. Figure 5 and Figure 6 compare the spatial distribution
294 of PM_{2.5} compositions, and similar overpredictions of PM_{2.5} compositions can be observed in the
295 mountain area in Northern China.

296 The ability of InMAP-China to predict PM_{2.5} compositions is also examined at various emission
297 levels. Figure 7 compares the concentrations of PM_{2.5} compositions and the proportions of secondary
298 inorganic aerosols (hereafter, SNA) in total PM_{2.5} concentrations in different scenarios by two models.
299 In the InMAP_TOT scenario, the proportion of SNA is 56%, which is extremely close to the 50%
300 proportion in the WRF-CMAQ simulations. In five emission abatement simulations, the proportion was
301 approximately equal to that in the baseline scenario because the linearly treated chemical reaction
302 relationship of SNA was employed in InMAP-China. However, focusing on the simulations of five
303 sectoral emission scenarios, a significant difference can be observed, which is mainly caused by the

304 difference in chemical treatments in InMAP-China and CMAQ. In this situation, the impacts on $PM_{2.5}$
305 concentrations are distinct due to the nonlinear emission-concentration process.

306 3.1.2 Marginal change in $PM_{2.5}$ concentrations

307 Figure 8 compares the InMAP-China and CMAQ predictions of population-weighted $PM_{2.5}$
308 concentrations and $PM_{2.5}$ compositions for eleven emission scenarios. Marginal changes in air pollutant
309 concentrations are defined as $1 \mu\text{g}/\text{m}^3$ by normalizing the population-weighted air pollutant
310 concentrations of each scenario using the largest value among all scenarios modelled by CMAQ. The
311 InMAP-China reproduces CMAQ predictions on the marginal change in population-weighted $PM_{2.5}$
312 concentrations, with a NMB of -12% and correlations of 0.98, as shown in Figure 8(a). This performance
313 is similar to that predicted by InMAP in the United States (Tessum et al., 2017).

314 Figure 8(b)-(f) compares the predictions of $PM_{2.5}$ compositions. The InMAP-China predictions of
315 SO_4^{2-} , NO_3^- , NH_4^+ and primary $PM_{2.5}$ agree well with the CMAQ results, but the predictions of secondary
316 organic aerosol (SOA) are the poorest. The marginal changes in NO_3^- and primary $PM_{2.5}$ concentrations
317 are moderately underpredicted by InMAP-China, with NMB values of -13% and -21%, respectively.
318 Conversely, the marginal change in SO_4^{2-} concentrations is overpredicted with an NMB of 23%. The
319 marginal change in NH_4^+ predicted by InMAP-China agrees well with the CMAQ predictions. Because
320 few reaction pathways of SOA are included in the CB05 mechanism in the CMAQ simulations, SOAs
321 are underpredicted in the entire modelling system.

322 The regional performance of the changes in $PM_{2.5}$ and its compositions for eleven emission
323 scenarios is also examined in this study. Figures S4-S7 show the regional results. Four regions, including
324 the Beijing-Tianjin-Hebei region (BTH), Yangtze River Delta (YRD), Pearl River Delta (PRD), and Fen
325 Wei Plain (FWP), are analysed here (see Figure 2). At the regional level, the CMAQ predicted marginal
326 changes in population-weighted $PM_{2.5}$ concentrations, and its composition can be reproduced by InMAP-
327 China, which is similar to the nationwide performance. However, the marginal change in SO_4^{2-}
328 concentrations over the BTH is significantly overpredicted by InMAP-China, with an NMB of 135%,
329 which is expected to be improved by optimizing the representation of the annual sulfate oxidation rate
330 in this region.

331 3.2 Model performance of source contributions

332 Figure 9 shows the contribution of each sector to $PM_{2.5}$ concentrations nationwide and at the regional
333 scale, and Table 4 displays the proportion value of sectoral contribution based on two models. The

334 predictions of the source contributions of PM_{2.5} concentrations in InMAP-China are basically reliable
335 compared with those based on the CMAQ model, and the difference can be explained.

336 The results based on the two models indicate that the industrial and residential sectors are the first
337 and second contributors among the five sectors. The contribution of the electricity sector is comparable
338 when using the two models, while the contributions of transportation and agriculture are moderately
339 different, which is mainly due to the difference in the model mechanism and the treatment of secondary
340 inorganic aerosols in the two models. At the regional scale, the difference in the sectoral contribution
341 caused by the mechanism in the two models is more significant than at the national scale.

342 3.3 Model performance of PM_{2.5}-related premature mortality

343 Figure 10 compares the predictions of PM_{2.5}-related premature mortality based on two models at
344 the provincial level. The PM_{2.5}-related premature mortality estimated using InMAP-China was 1.92
345 million people in 2017. Compared with the CMAQ-based estimations, 25 ten thousand deaths are under-
346 predicted by InMAP-China because of underestimation of total PM_{2.5} concentrations in the baseline
347 simulation. At the provincial level, the PM_{2.5}-related premature mortality in Beijing city, Tianjin city,
348 Hebei province and Shanghai city is slightly overpredicted by InMAP-China, with the relative difference
349 ranging from 4% to 15%. Conversely, for the other majority of provinces, PM_{2.5}-related premature
350 mortality is under-predicted by InMAP-China, with the relative difference ranging from -3% to -44%.

351 4 Conclusions

352 This work develops a reduced-complexity air quality intervention model over China and presents a
353 comprehensive evaluation by comparing CMAQ simulations and surface observations. InMAP-China
354 has the advantage of being time-efficient in conducting air quality predictions and health impact
355 assessments of emission sources in China.

356 InMAP-China performed well for the prediction of PM_{2.5} concentrations. The model satisfactorily
357 predicts total PM_{2.5} concentrations in the baseline simulation in terms of statistical performance.
358 Compared with the observed PM_{2.5} concentrations, the MB, NMB, and correlations of the total PM_{2.5}
359 concentrations are -8.1 µg/m³, -18%, and 0.6, respectively. The statistical performance is satisfactory for
360 a reduced-complexity air quality model and remains consistent with the performance evaluation in the
361 United States. The underestimation of total PM_{2.5} mainly comes from the primary PM_{2.5}. Moreover, the
362 spatial pattern of total PM_{2.5} concentrations can be reproduced in InMAP-China, while an overestimation

363 over the mountain area in Northern China can be observed. The large emission intensity and complex
364 terrain over this region increase the difficulty of modelling concentrations in this area. The predictions
365 of source contributions to PM_{2.5} concentrations by InMAP-China are comparable with those based on
366 the CMAQ model, and the difference is mainly caused by the uncertainty of the simplification of
367 chemical process in the InMAP-China. Focusing on the predictions of health impacts, InMAP-China
368 shows moderate under-predictions of 25 ten thousand people deaths compared with CMAQ-based
369 predictions due to the underestimation of total PM_{2.5} concentrations.

370 Although the modelling system has an acceptable performance, research work is suggested to
371 further improve the model performance. This study is subject to some limitations and uncertainties. In
372 InMAP-China, the annual-average chemical and physical processes parameters are calculated using
373 hourly parameters from WRF-CMAQ. Complicated seasonal and daily variations affecting the formation
374 and transportation of particulate matter are challenging to retain. The intensity of advection of the air
375 mass is supposed to be weakened due to the offset of the wind vector in the averaging process, which
376 was also pointed out in a previous study. Moreover, InMAP-China has difficulty predicting SOA
377 concentrations because reaction pathways for SOA are insufficient in this modelling system.

378 The development of InMAP-China aims at providing an alternative to the conventional CTMs to
379 predicting the PM_{2.5} concentrations due to emission change in the mainland of China. InMAP-China has
380 the advantage of time efficiency and a satisfactory performance in this study; however, this model has a
381 modest reduction in accuracy compared with conventional CTMs; hence, some limitations still exist for
382 model applications. In terms of the applicability of this modelling system, we recommend users to select
383 InMAP-China as a prior tool with the following objectives: quantification of the contribution of multiple
384 emission sources in baseline atmospheric conditions, for instance, the PM_{2.5} air quality and health impacts
385 contributed by dozens of categories of fine emission sources, and rapid estimation of the general air
386 quality and health benefits attributable to a series of control policies. Instead, if the objective of
387 simulations is to predict the actual situation and pre-estimate the reductions in PM_{2.5} concentrations due
388 to control measures, conventional CTMs are a better choice because the change in atmospheric
389 conditions along with emission change should be taken into account.

390

删除的内容: The development of InMAP-China aims at providing an alternative to the conventional CTMs to predicting the PM_{2.5} concentrations due to emission change in the mainland of China.

395 **Code and data availability**

396 The source code for the localized version of reduced-complexity air quality model over China (InMAP-
397 China), which is developed based on the original InMAP model over the United states. The data related
398 to this study as well as the user manual are available at <https://doi.org/10.5281/zenodo.5111961>.

399 **Author contributions**

400 RL. Wu and Q. Zhang designed the research and RL. Wu carried them out. RL. Wu, CW. Tessum and
401 Y. Zhang contributed to model development. RL. Wu prepared the manuscript with contributions from
402 all co-authors.

403 **Competing interests**

404 The authors declare no competing interests.

405 **Acknowledgements**

406 This work was supported by the National Natural Science Foundation of China (41921005 and
407 41625020). And this work was also funded under Assistance Agreement No. RD835871 awarded by the
408 U.S. EPA to Yale University. The views expressed in this manuscript are those of the authors alone and
409 do not necessarily reflect the views and policies of the U.S. EPA. The EPA does not endorse any products
410 or commercial services mentioned in this publication.

411

412

413

414

415

416

417

418

删除的内容: The source code for the localized version of reduced-complexity air quality model over China (InMAP-China), which is developed based on the original InMAP model over the United states. The data related to this study as well as the user manual are available at <https://doi.org/10.5281/zenodo.5111961>.

425 **References**

426 A. Xiu, J. E. Pleim. Development of a Land Surface Model. Part I: Application in a Mesoscale
427 Meteorological Model. *Journal of Applied Meteorology*, 40:192-209, 2011.

428 Appel, K.W., Napelenok, S.L., Hogrefe, C., Foley, K.M., Pouliot, G.A., Murphy, B., Heath, N., Roselle,
429 S., Pleim, J., Bash, J.O., Pye, H.O.T., Mathur, R. Overview and evaluation of the Community Multiscale
430 Air Quality (CMAQ) modelling system version 5.2. *Air Pollution Modelling and its Application XXV*,
431 11:63-72. ITM 2016. Springer Proceedings in Complexity. Springer, Cham, doi: 10.1007/978-3-319-
432 57645-9_11, 2017.

433 Appel, K.W., Napelenok, S.L., Hogrefe, C., Foley, K.M., Pouliot, G.A., Murphy, B., Heath, N., Roselle,
434 S., Pleim, J., Bash, J.O., Pye, H.O.T., Mathur, R. Overview and evaluation of the Community Multiscale
435 Air Quality (CMAQ) modelling system version 5.2. *Air Pollution Modelling and its Application XXV*,
436 11:63-72. ITM 2016. Springer Proceedings in Complexity. Springer, Cham, doi: 10.1007/978-3-319-
437 57645-9_11, 2017.

438 Baker, K. R.; Amend, M.; Penn, S.; Bankert, J.; Simon, H.; Chan, E.; Fann, N.; Zawacki, M.; Davidson,
439 K.; Roman, H., A database for evaluating the InMAP, APEEP, and EASIUR reduced complexity air-
440 quality modelling tools. *Data in Brief*, 28, 2020.

441 Burnett, R.; Chen, H.; Szyszkowicz, M.; Fann, N.; Hubbell, B.; Pope, C. A.; Apte, J. S.; Brauer, M.;
442 Cohen, A.; Weichenthal, S.; Coggins, J.; Di, Q.; Brunekreef, B.; Frostad, J.; Lim, S. S.; Kan, H. D.;
443 Walker, K. D.; Thurston, G. D.; Hayes, R. B.; Lim, C. C.; Turner, M. C.; Jerrett, M.; Krewski, D.; Gapstur,
444 S. M.; Diver, W. R.; Ostro, B.; Goldberg, D.; Crouse, D. L.; Martin, R. V.; Peters, P.; Pinault, L.;
445 Tjepkema, M.; Donkelaar, A.; Villeneuve, P. J.; Miller, A. B.; Yin, P.; Zhou, M. G.; Wang, L. J.; Janssen,
446 N. A. H.; Marra, M.; Atkinson, R. W.; Tsang, H.; Thach, Q.; Cannon, J. B.; Allen, R. T.; Hart, J. E.;
447 Laden, F.; Cesaroni, G.; Forastiere, F.; Weinmayr, G.; Jaensch, A.; Nagel, G.; Concin, H.; Spadaro, J.
448 V., Global estimates of mortality associated with long-term exposure to outdoor fine particulate matter.
449 *Proceedings of the National Academy of Sciences of the United States of America*, 115, (38), 9592-9597,
450 2018.

451 C. J. Walcek, Taylor GR. A Theoretical Method for Computing Vertical Distributions of Acidity and
452 Sulfate Production within Cumulus Clouds. *Journal of the Atmospheric Science*, 43:339-55, 1986.

删除的内容: Journal of the Atmospheric Science

454 Chang, X.; Wang, S.; Zhao, B.; Xing, J.; Liu, X.; Wei, L.; Song, Y.; Wu, W.; Cai, S.; Zheng, H.; Ding,
455 D.; Zheng, M., Contributions of inter-city and regional transport to PM_{2.5} concentrations in the Beijing-
456 Tianjin-Hebei region and its implications on regional joint air pollution control. *Science of the Total*
457 *Environment*, 660, 1191-1200, 2019.

458 Cohen, A. J.; Brauer, M.; Burnett, R.; Anderson, H. R.; Frostad, J.; Estep, K.; Balakrishnan, K.;
459 Brunekreef, B.; Dandona, L.; Dandona, R.; Feigin, V.; Freedman, G.; Hubbell, B.; Jobling, A.; Kan, H.;
460 Knibbs, L.; Liu, Y.; Martin, R.; Morawska, L.; Pope, C. A., III; Shin, H.; Straif, K.; Shaddick, G.; Thomas,
461 M.; van Dingenen, R.; van Donkelaar, A.; Vos, T.; Murray, C. J. L.; Forouzanfar, M. H., Estimates and
462 25-year trends of the global burden of disease attributable to ambient air pollution: an analysis of data
463 from the Global Burden of Diseases Study 2015. *Lancet* 389, (10082), 1907-1918, 2017.

464 Dimanchevi, E. G.; Paltsev, S.; Yuan, M.; Rothenberg, D.; Tessum, C. W.; Marshall, J. D.; Selin, N. E.,
465 Health co-benefits of sub-national renewable energy policy in the US. [Environmental Research Letters](#),
466 14, (8), 2019.

467 Doxsey-Whitfield E, MacManus K, Adamo S B, Susana B, Pistolesi L, Squires J, Borkovska O and
468 Baptista S R Taking advantage of the improved availability of census data: a first look at the gridded
469 population of the world, version 4. *Papers in Applied Geography*. 1 226–34, 2015.

470 E. J. Mlawer, S. J. Taubman, P. D. Brown, M. J. Iacono, S. A. Clough. Radiative transfer for
471 inhomogeneous atmospheres: RRTM, a validated correlated-k model for the longwave. [Journal of](#)
472 [Geophysical Research](#), 102:16663-82, 1997.

473 Fountoukis C and Nenes A. ISORROPIA II: A Computationally Efficient Aerosol Thermodynamic
474 Equilibrium Model for K⁺, Ca²⁺, Mg²⁺, NH₄⁺, Na⁺, SO₄²⁻, NO₃⁻, Cl⁻, H₂O Aerosols, [Atmospheric](#)
475 [Chemistry Physics](#), 7, 4639-4659, 2007.

476 Gilmore, E. A.; Heo, J.; Muller, N. Z.; Tessum, C. W.; Hill, J. D.; Marshall, J. D.; Adams, P. J., An inter-
477 comparison of the social costs of air quality from reduced-complexity models. *Environmental Research*
478 *Letters*, 14, (7), 2019.

479 Global Burden of Disease Collaborative Network. Global Burden of Disease Study 2017 (GBD 2017)
480 Population Estimates 1950-2017. Seattle, United States: Institute for Health Metrics and Evaluation
481 (IHME), 2018.

删除的内容: Environmental Research Letters

删除的内容: Journal of Geophysical Research

删除的内容: Atmospheric Chemistry Physics

485 Global Burden of Disease Collaborative Network. Global Burden of Disease Study 2017 (GBD 2017)
486 Cause-Specific Mortality 1980-2017. Seattle, United States: Institute for Health Metrics and Evaluation
487 (IHME), 2018.

488 Goodkind AL, Tessum CW, Coggins JS, Hill JD, Marshall JD. Fine-scale damage estimates of particulate
489 matter air pollution reveal opportunities for location-specific mitigation of emissions. Proceedings of the
490 National Academy of Sciences. Apr 3:201816102. <https://doi.org/10.1073/pnas.1816102116>, 2019.

491 Guenther, A. B.; Jiang, X.; Heald, C. L.; Sakulyanontvittaya, T.; Duhl, T.; Emmons, L. K.; Wang, X.,
492 The Model of Emissions of Gases and Aerosols from Nature version 2.1 (MEGAN2.1): an extended and
493 updated framework for modelling biogenic emissions. Geoscientific Model Development Discussions,
494 5, (2), 1503-1560, 2012.

495 Heo, J.; Adams, P. J.; Gao, H. O., Public health costs accounting of inorganic PM_{2.5} pollution in
496 metropolitan areas of the United States using a risk-based source-receptor model. Environment
497 International, 106, 119-126, 2017.

498 Heo, J.; Adams, P. J.; Gao, H. O., Reduced-form modelling of public health impacts of inorganic PM_{2.5}
499 and precursor emissions. Atmospheric Environment, 137, 80-89, 2016.

500 Hong, C.; Zhang, Q.; Zhang, Y.; Tang, Y.; Tong, D.; He, K., Multi-year downscaling application of two-
501 way coupled WRF v3.4 and CMAQ v5.0.2 over east Asia for regional climate and air quality modelling:
502 model evaluation and aerosol direct effects. Geoscientific Model Development, 10, (6), 2447-2470, 2017.

503 J. E. Pleim. A Combined Local and Nonlocal Closure Model for the Atmospheric Boundary Layer. Part
504 I: Model Description and Testing. Journal of Applied Meteorology and Climatology, 46:1383-95, 2007.

505 J. S. Chang, R. A. Brost, I. S. A. Isaksen, S. Madronich, P. Middleton, W. R. Stockwell, et al. A three-
506 dimensional Eulerian acid deposition model: Physical concepts and formulation. [Journal of Geophysical](#)
507 [Research](#), 92:14681-700, 1987.

508 J. S. Kain. The Kain-Fritsch Convective Parameterization: An Update. Journal of Applied Meteorology.
509 2004, 43:170-81.

510 Li, M.; Zhang, Q.; Kurokawa, J.-i.; Woo, J.-H.; He, K.; Lu, Z.; Ohara, T.; Song, Y.; Streets, D. G.;
511 Carmichael, G. R.; Cheng, Y.; Hong, C.; Huo, H.; Jiang, X.; Kang, S.; Liu, F.; Su, H.; Zheng, B., MIX:
512 a mosaic Asian anthropogenic emission inventory under the international collaboration framework of the

删除的内容: Journal of Geophysical Research

514 MICS-Asia and HTAP. *Atmospheric Chemistry and Physics*, 17, (2), 935-963, 2017.

515 Li, X.; Zhang, Q.; Zhang, Y.; Zheng, B.; Wang, K.; Chen, Y.; Wallington, T. J.; Han, W.; Shen, W.; Zhang,
516 X.; He, K., Source contributions of urban PM_{2.5} in the Beijing-Tianjin-Hebei region: Changes between
517 2006 and 2013 and relative impacts of emissions and meteorology. *Atmospheric Environment*, 123, 229-
518 239, 2015.

519 Liu, F.; Zhang, Q.; Tong, D.; Zheng, B.; Li, M.; Huo, H.; He, K. B., High-resolution inventory of
520 technologies, activities, and emissions of coal-fired power plants in China from 1990 to 2010.
521 *Atmospheric Chemistry and Physics*, 15, (23), 13299-13317, 2015.

522 M.-D. Chou, M. J. Suarez, C.-H. Ho, M. M.-H. Yan, K.-T. Lee. Parameterizations for Cloud Overlapping
523 and Shortwave Single-Scattering Properties for Use in General Circulation and Cloud Ensemble Models.
524 *Journal of Climate*, 11:202-14, 1998.

525 Muller, N. Z., Mendelsohn, R. Measuring the damages of air pollution in the United States. *Journal of*
526 *Environmental Economics and Management*, 54(1), 1–14. <https://doi.org/10.1016/j.jeem.2006.12.002>,

527 Muller, N. Z., Mendelsohn, R., & Nordhaus, W. Environmental accounting for pollution in the United
528 States economy. *American Economic Review*, 101(5), 1649-75. DOI:10.1257/aer.101.5.1649, 2011.

529 Multi-resolution Emission Inventory of China (<http://meicmodel.org/>).

530 National Centers for Environmental Prediction/National Weather Service/NOAA/US Department of
531 Commerce NCEP FNL Operational Model Global Tropospheric Analyses, continuing from July 1999
532 Dataset (<https://doi.org/10.5065/D6M043C6>), 2000.

533 Reddington, C. L.; Conibear, L.; Knote, C.; Silver, B.; Li, Y. J.; Chan, C. K.; Arnold, S. R.; Spracklen,
534 D. V., Exploring the impacts of anthropogenic emission sectors on PM_{2.5} and human health in South and
535 East Asia. *Atmospheric Chemistry and Physics*, 19, (18), 11887-11910, 2019.

536 Sergi, B. J.; Adams, P. J.; Muller, N. Z.; Robinson, A. L.; Davis, S. J.; Marshall, J. D.; Azevedo, I. L.,
537 Optimizing Emissions Reductions from the U.S. Power Sector for Climate and Health Benefits.
538 *Environmental science & technology*, 54, (12), 7513-7523, 2020.

539 Skamarock W, Klemp J, Dudhia J, Gill D, Barker D, Duda M, Huang X, Wang Wand Powers J A
540 description of the Advanced Research WRF Version 3 NCAR technical note (Boulder, CO: National
541 Center for Atmospheric Research), 2008.

542 Tessum, C. W.; Hill, J. D.; Marshall, J. D., InMAP: A model for air pollution interventions. *PLoS One*,
543 12, (4), e0176131, 2017.

544 Thind, M. P. S.; Tessum, C. W.; Azevedo, I. L.; Marshall, J. D., Fine Particulate Air Pollution from
545 Electricity Generation in the US: Health Impacts by Race, Income, and Geography. *Environmental*
546 *Science & Technology*, 53, (23), 14010-14019, 2019.

547 United States Environmental Protection Agency. National Emission Inventory data.
548 <https://www.epa.gov/air-emissions-inventories/2011-national-emissions-inventory-nei-data>. 2011.

549 Whitten G Z, Heo G, Kimura Y, et al. A new condensed toluene mechanism for Carbon Bond CB05-TU.
550 *Atmospheric Environment*, 44(40SI):5346-5355, 2010.

551 Wu, R.; Liu, F.; Tong, D.; Zheng, Y.; Lei, Y.; Hong, C.; Li, M.; Liu, J.; Zheng, B.; Bo, Y.; Chen, X.; Li,
552 X.; Zhang, Q., Air quality and health benefits of China's emission control policies on coal-fired power
553 plants during 2005–2020. *Environmental Research Letters*, 14, (9), 094016, 2019.

554 Xiao, Q. Y.; Geng, G. N.; Liang, F. C.; Wang, X.; Lv, Z.; Lei, Y.; Huang, X. M.; Zhang, Q.; Liu, Y.; He,
555 K., Changes in spatial patterns of PM_{2.5} pollution in China 2000–2018: Impact of clean air policies.
556 *Environment international*, 141, 105776, 2020.

557 Zhang, L.; Liu, L. C.; Zhao, Y. H.; Gong, S. L.; Zhang, X. Y.; Henze, D. K.; Capps, S. L.; Fu, T. M.;
558 Zhang, Q.; Wang, Y. X., Source attribution of particulate matter pollution over North China with the
559 adjoint method. *Environmental Research Letters*, 10, (8), 2015.

560 Zhang, Q.; Zheng, Y.; Tong, D.; Shao, M.; Wang, S.; Zhang, Y.; Xu, X.; Wang, J.; He, H.; Liu, W.; Ding,
561 Y.; Lei, Y.; Li, J.; Wang, Z.; Zhang, X.; Wang, Y.; Cheng, J.; Liu, Y.; Shi, Q.; Yan, L.; Geng, G.; Hong,
562 C.; Li, M.; Liu, F.; Zheng, B.; Cao, J.; Ding, A.; Gao, J.; Fu, Q.; Huo, J.; Liu, B.; Liu, Z.; Yang, F.; He,
563 K.; Hao, J., Drivers of improved PM_{2.5} air quality in China from 2013 to 2017. *Proceedings of the*
564 *National Academy of Sciences of the United States of America*, 116, (49), 24463-24469, 2019.

565 Zheng, B.; Zhang, Q.; Zhang, Y.; He, K. B.; Wang, K.; Zheng, G. J.; Duan, F. K.; Ma, Y. L.; Kimoto, T.,
566 Heterogeneous chemistry: a mechanism missing in current models to explain secondary inorganic aerosol
567 formation during the January 2013 haze episode in North China. *Atmospheric Chemistry and Physics*,
568 15, (4), 2031-2049, 2015.

569

570 **Table 1. Model configurations in InMAP-China.**

Category	Parameters	Configurations
Basic	Research area and period	China, 2017
	Spatial resolution	36 km × 36 km
	Vertical layers	14 layers
	Run type	Steady run
	Variable grid	Static grid
	Projection	Lambert
	Grid numbers	305816
	Meteorological and chemical parameters	Calculated using variables from WRFv3.8-CMAQv5.2
Input	Anthropogenic emissions	MEIC, MIX, MEGAN
	Population data	GPW 2015 and GBD 2017
	Baseline mortality rate	GBD 2017
Output	Air pollutants	PM _{2.5} and its composition concentrations
	Mortality	PM _{2.5} -related premature mortality

571

572

573

574

575

576

577

578

579

580

Table 2 The relationship between parameters for simplified simulation and original variables.

带格式表格

WRF-CMAQ's Variables	Descriptions	InMAP-China's Parameters	Descriptions
U, V, W	Wind fields	UAvg, UDeviation VAvg, VDeviation WAvg, WDeviation	Advection and mixing coefficients
PH, PHB	Base state of geopotential and perturbation geopotential	Dz	Layer heights
PBLH	Planetary boundary layer height	M2d, M2u, Kxxyy, Kzz	Mixing coefficients
T	Potential Temperature	SO ₂ Oxidation, PlumeHeight	Chemical reaction rates and plume rise
P, PB	Base state pressure plus perturbation pressure		Chemical reaction rates and plume rise
QRAIN	Mixing ratio of rain	ParticleWetdep, GasWetdep	Wet deposition
QCLOUD	Cloud mixing ratio	SO ₂ Oxidation	Aqueous-phase chemical reaction rates
CLDFRA	Fraction of grid cell covered by clouds	ParticleWetdep, GasWetdep	Wet deposition
SWDOW N, GLW	Downward shortwave and longwave radiative flux at ground level	GasDrydep, ParticleWetdep	Dry deposition
HFX	Surface heat flux	M2d, M2u, Kxxyy, Kzz, Drydep	Mixing and dry deposition
UST	Friction velocity		Mixing and dry deposition
LU_INDE X	Land use type	M2d, M2u, Kxxyy, Kzz	Mixing
DENS	Inverse air density		Mixing and convert between mixing ratio and mass concentration
aVOC	Anthropogenic VOCs that are SOA precursors	aOrgPartitioning	VOCs/SOA partitioning
aSOA	Anthropogenic SOA		
OH, H ₂ O ₂	Hydroxyl radical and hydrogen peroxide concentrations	SO ₂ Oxidation	Oxidation rates
pNO	ANO ₃ I, ANO ₃ J	NOPartitioning	

gNO	NO and NO ₂		NO _x /pNO ₃ partitioning
pNH	ANH ₄ I, ANH ₄ J	NHPartitioning	NH ₃ /pNH ₄ partitioning
gNH	NH ₃		

582
583
584
585
586
587
588
589
590
591
592
593
594
595
596
597
598
599
600
601
602
603
604
605

606 **Table 3 Simulation experiments conducted using InMAP-China.**

Class	Simulations	Emission input	Physical and chemical parameter input
Sec1	InMAP_POW	Power plants emissions	
Sec2	InMAP_INDUS	Industrial emissions	
Sec3	InMAP_TRANS	Transportation emissions	
Sec4	InMAP_RESI	Residential emissions	
Sec5	InMAP_AGRI	Agricultural emissions	
BASE	InMAP_TOT	Five sectoral anthropogenic emissions and natural emissions	
Aba1	InMAP_RE10	Reduce the air pollutants emissions by 10% based on InMAP_TOT emissions	
Aba2	InMAP_RE30	Reduce the air pollutants emissions by 30% based on InMAP_TOT emissions	
Aba3	InMAP_RE50	Reduce the air pollutants emissions by 50% based on InMAP_TOT emissions	Converted using WRF-CMAQv5.2 simulation data in the year of 2017;
Aba4	InMAP_RE70	Reduce the air pollutants emissions by 70% based on InMAP_TOT emissions	Remain the same in all simulations.
Aba5	InMAP_RE90	Reduce the air pollutants emissions by 90% based on InMAP_TOT emissions	

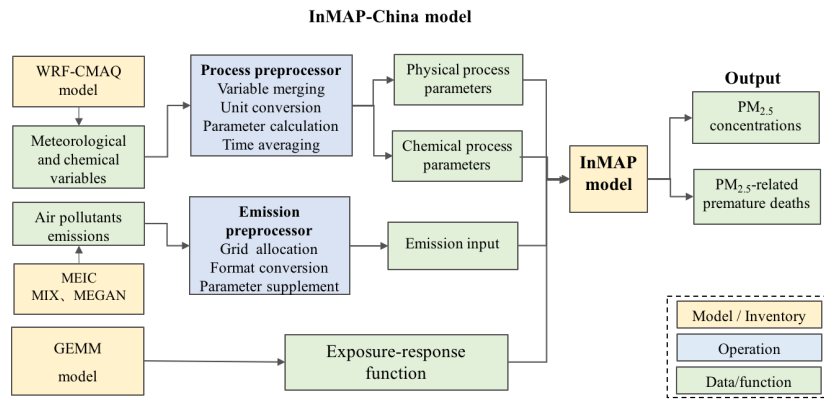
删除的内容: CMAQv5.2

607
608
609
610
611
612
613
614
615

617 **Table 4 Comparison of the proportions of sectoral contributions to PM_{2.5} concentrations using InMAP-**
 618 **China and CMAQ.**

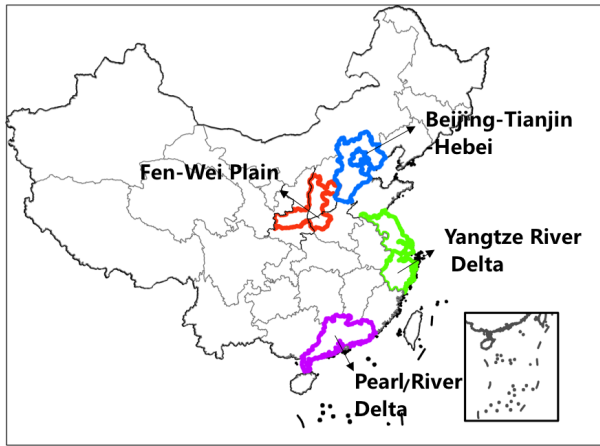
Sector	National		BTH		YRD		PRD		FWPY	
	CMAQ	InMAP- P- China	CMAQ	InMAP- P- China	CMAQ	InMAP- P- China	CMAQ	InMAP- P- China	CMAQ	InMAP- P- China
Power	6.9%	8.1%	6.2%	9.4%	7.4%	8.6%	10.4%	8.2%	7.0%	10.0%
Industry	30.8%	35.0%	30.2%	38.2%	33.3%	39.1%	37.5%	35.4%	27.7%	31.9%
Residential	25.9%	28.1%	24.7%	28.2%	17.9%	20.8%	19.5%	28.4%	30.0%	33.8%
Transportation	14.0%	17.3%	13.4%	15.6%	15.7%	21.2%	17.1%	17.5%	13.2%	15.0%
Agriculture	22.5%	11.5%	25.5%	10.4%	25.7%	12.4%	15.4%	11.6%	22.0%	9.4%

619
 620
 621
 622
 623
 624
 625
 626
 627
 628
 629
 630
 631



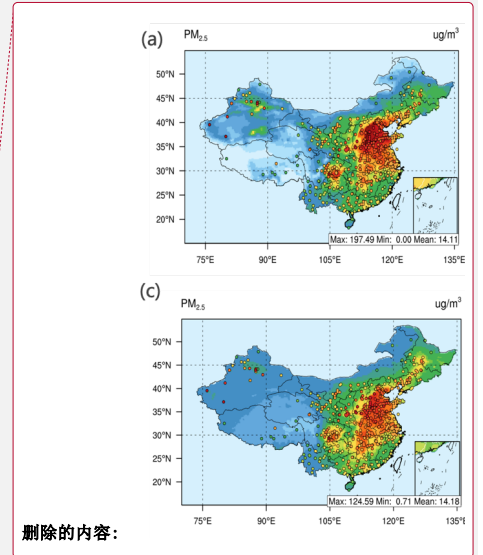
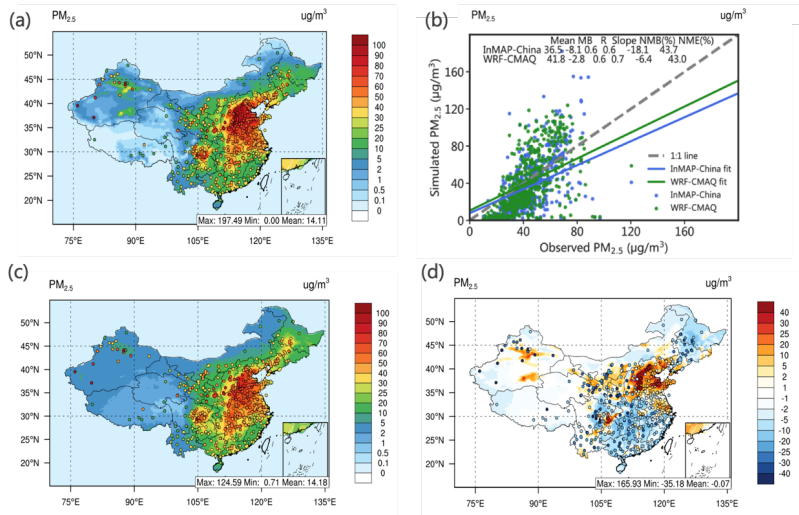
632
633 **Figure 1 Model framework of InMAP-China.**

634
635
636
637
638
639
640
641
642
643
644
645
646
647

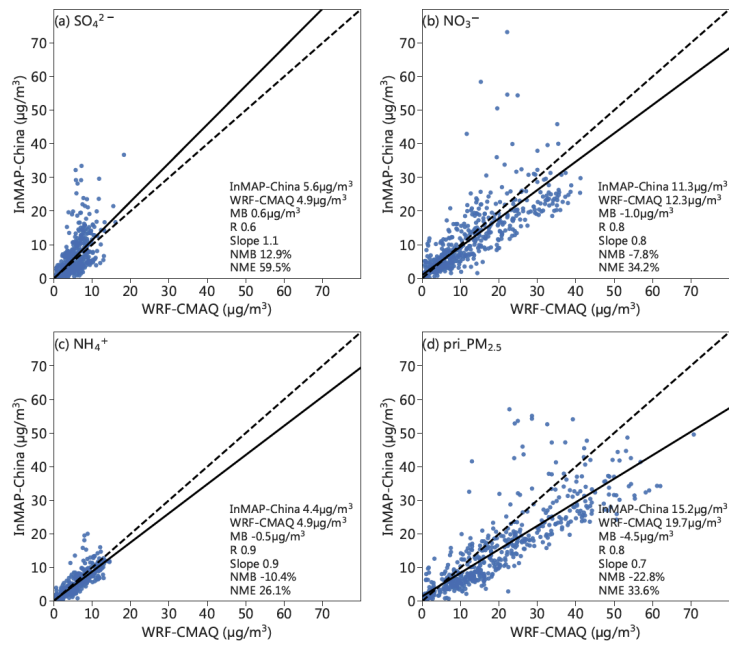


648
649 **Figure 2** Four key regions defined in this study, including the Beijing-Tianjin-Hebei region, Yangtze River
650 Delta region, Pearl River Delta region and Fen Wei Plain region.

651
652
653
654
655
656
657
658
659
660
661



662
 663 **Figure 3 The spatial pattern and statistical metrics of total $PM_{2.5}$ concentrations predicted by InMAP-China**
 664 **and WRF-CMAQ.** Panels (a) and (c) display the spatial patterns of total $PM_{2.5}$ concentrations predicted by InMAP-
 665 China and WRF-CMAQ, respectively. Panel (d) presents the difference in the spatial distribution of the total $PM_{2.5}$
 666 concentrations predicted by the two models. Panel (b) shows the statistical metrics between the simulated and
 667 observed $PM_{2.5}$. The observed total $PM_{2.5}$ concentrations are marked as circles in panel (a) and panel (c). In panel
 668 (d), the circle shows the difference between the $PM_{2.5}$ simulated by InMAP-China and the observed $PM_{2.5}$. The same
 669 colorbar is utilized in the contour and the marked circle.

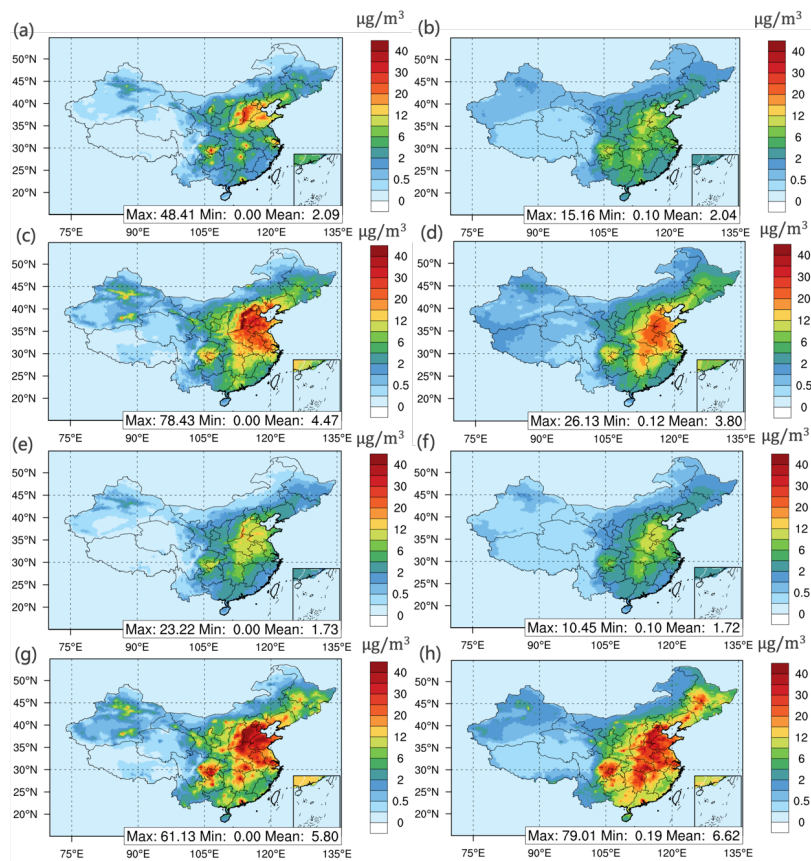


671

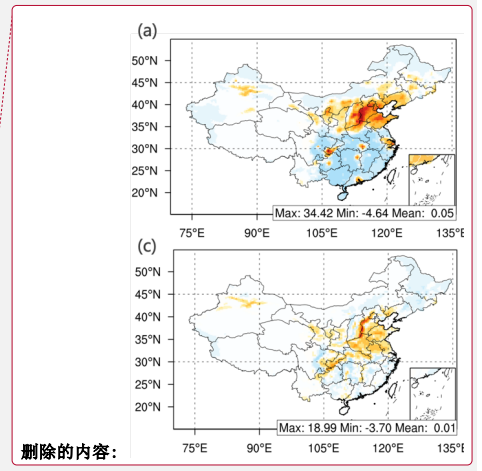
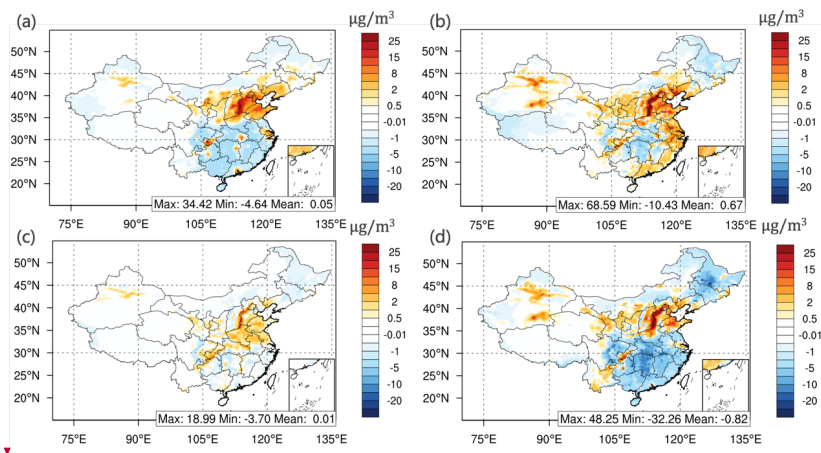
672 **Figure 4** Scatter plot comparing the PM_{2.5} composition concentration modelled by the InMAP-China and

673 **WRF-CMAQ models.** Panels (a), (b), (c) and (d) display sulfate, nitrate, ammonium, and primary PM_{2.5},

674 respectively. The statistical metrics are labelled in the lower right corner in each panel.



675
 676 **Figure 5** The spatial pattern of PM_{2.5} compositions modelled by the InMAP-China and WRF-CMAQ models.
 677 Panels (a), (c), (e), and (g) present the sulfate, nitrate, ammonium, and primary PM_{2.5}, respectively, simulated by
 678 InMAP-China in the InMAP-TOT scenario. Panels (b), (d), (f), and (h) present the results modelled by WRF-CMAQ.



679

680 **Figure 6** The difference in the spatial pattern of $PM_{2.5}$ compositions between InMAP-China and WRF-CMAQ.

681 Panels (a), (b), (c), and (d) display sulfate, nitrate, ammonium, and primary $PM_{2.5}$, respectively.

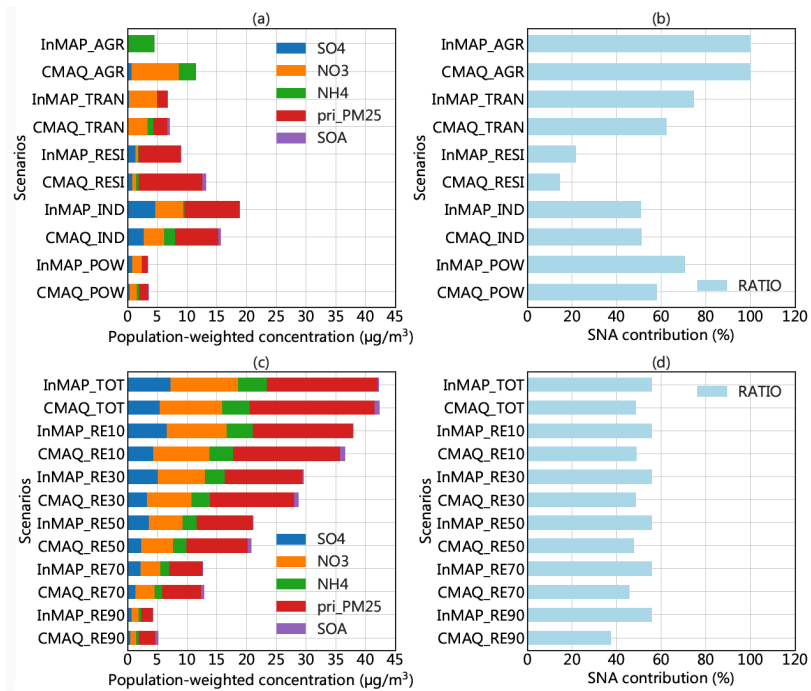
682

683

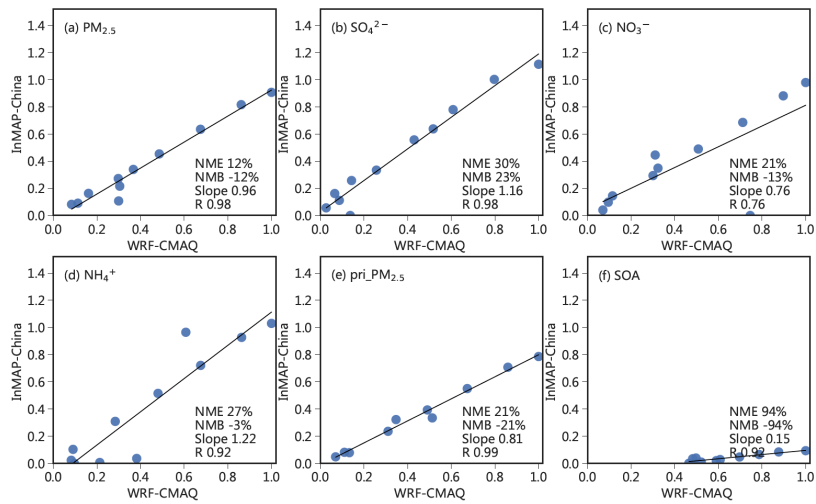
684

685

686

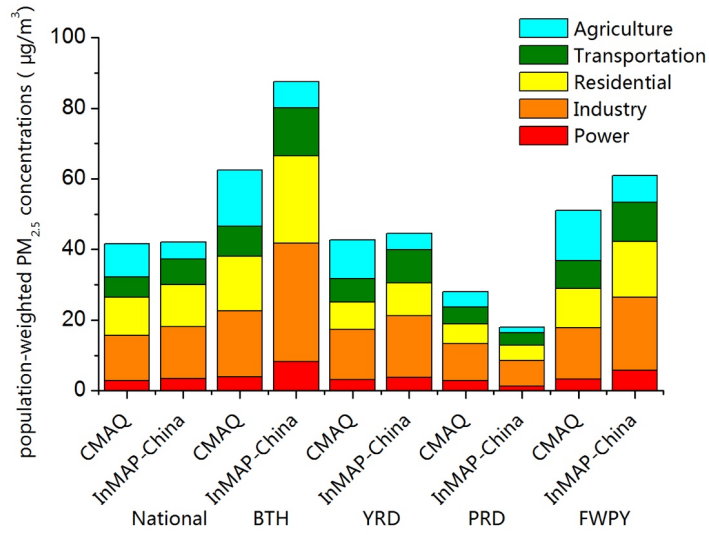


688
 689 **Figure 7 Comparison of PM_{2.5} component concentrations and SNA contributions in these eleven simulations.**
 690 (a) and (c) show the modelled PM_{2.5} compositions. Panel (a) presents the results of sectoral emission scenarios, and
 691 panel (c) presents the results of the baseline and emission abatement scenarios. Panels (b) and (d) present the SNA
 692 contribution (%) for each scenario.



693
 694 **Figure 8 Marginal change in nationwide annual average population-weighted $PM_{2.5}$ concentration and its**
 695 **composition as modelled by InMAP-China and WRF-CMAQ for eleven emissions scenarios.** The population-
 696 weighted pollutant concentration for each scenario is normalized using the largest value among all scenarios
 697 modelled by CMAQ. The eleven dots represent the eleven scenarios, and the statistical metrics are labelled in the
 698 lower right corner for each panel.

699
 700
 701



702

703 **Figure 9 Comparison of source contributions to population-weighted PM_{2.5} concentrations estimated by the**
 704 **two models.**

705

706

707

708

709

710

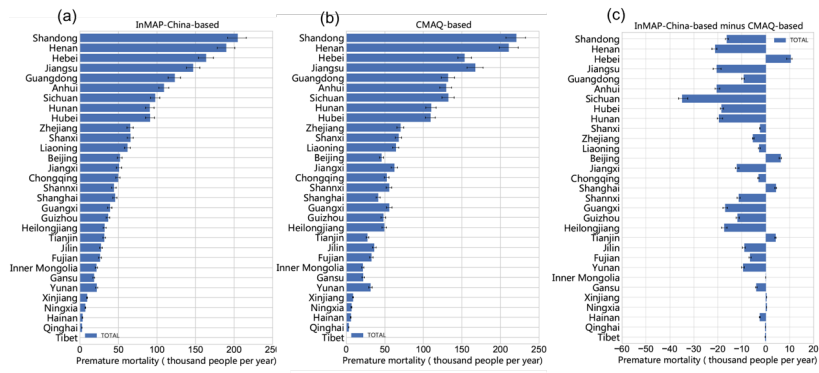
711

712

713

714

715



716
 717 **Figure 10 Comparison of PM_{2.5}-related premature mortality based on two models. (a) InMAP-China-based;**
 718 **(b) CMAQ-based; and (c) difference between the two models.**

719
 720
 721
 722
 723
 724
 725
 726
 727
 728
 729
 730
 731
 732
 733
 734